We now use the following formulas[9]:

$$Y_l^m(\hat{p})=\left(\frac{2l+1}{4\pi}\right)^{1/2}\left(\frac{(l-m)!}{(l+m)!}\right)^{1/2}\times(-1)^{l+m}e^{im\phi}P_l^m(\cos\theta)\,, \quad \text{(A5)}$$

$$J_m(ka\sin\theta)=\frac{1}{2\pi}\int_0^{2\pi}e^{+im\phi}e^{-ika\sin\theta\sin\phi}d\phi\,, \quad \text{(A6)}$$

$$e^{ka\cos\theta}J_m(ka\sin\theta)=(-1)^m\sum_{n=0}^{\infty}\frac{(ka)^{m+n}}{(2m+n)!}P_{n+m}^m(\cos\theta)\,, \quad \text{(A7)}$$

and one finds that

$$|d_{lm}(k,a)|^2=4\pi\left(\frac{a}{\pi k}\right)^{3/2}\frac{(ka)^{2l}}{(l+m)!(l-m)!}e^{-2ka}. \quad \text{(A8)}$$

Since

$$\sum_{m=-l}^{l}\binom{2l}{l+m}=2^{2l}\,, \quad \text{(A9)}$$

we have

$$f_l(k,a)=4\pi\left(\frac{a}{\pi k}\right)^{3/2}\frac{(2ka)^{2l}}{(2l)!}e^{-2ka}. \quad \text{(A10)}$$

For large l, Stirling's formula yields the estimate

$$f_l(k,a)\approx4\pi\left(\frac{a}{\pi k}\right)^{3/2}\frac{(2ka)^{2l}}{(2l)^{2l}e^{-2l}(2\pi 2l)^{1/2}}e^{-2ka}. \quad \text{(A11)}$$

For fixed l and k, f_l is maximized when

$$a=(l+\tfrac{3}{4})/k\,, \quad \text{(A12)}$$

and then

$$f_l\approx \text{const}\,l/k^3\,, \quad \text{(A13)}$$

which completes the proof.

[9] For (A6) and (A7) see G. N. Watson, *A Treatise on the Theory of Bessel Functions* (Cambridge University Press, New York, 1952), 2nd ed., pp. 31, 149, and the *Batemen Manuscript Project* (McGraw-Hill Book Company, Inc., New York, 1953), Vol. II, p. 182.

PHYSICAL REVIEW VOLUME 155, NUMBER 5 25 MARCH 1967

Interpretation of the N^* Effect in Deuteron Compton Scattering*

MELVIN MONTH

Department of Physics, University of Illinois, Urbana, Illinois

(Received 18 July 1966; revised manuscript received 10 October 1966)

Calculations of deuteron Compton scattering based on impulse methods demonstrate a peaking of the energy distributions due to the N^* pole in the factored nucleon amplitude. It is suggested here that the factorization procedure is questionable when a pole exists in the factored amplitude, as is evidenced, for example, by the failure of the procedure near threshold where the nucleon pole term is of importance. This difficulty is obviated in this paper by correctly treating the N^* as an intermediate state. It is shown that there exists a singularity which extends into the so-called anomalous region, very close to the physical scattering domain. This Landau singularity, manifested in a diagram having four propagators, has the effect of simulating a resonance-like behavior just above the N^*-nucleon threshold. However, this "resonance" has the interesting properties that as the deuteron momentum transfer increases, its effective width enlarges, while the peak height substantially diminishes. Using the dominance of the above-mentioned singularity as the basis for a computation, an expression for the deuteron Compton differential cross section was derived. To avoid ambiguities inherent in the spin case, scalar particles were used. A comparison with the limited experimental data available above the photopion threshold produced very encouraging results. However, to further clarify the manner in which the N^* manifests itself, it is suggested that attempts be made to extend the experiments (1) to a photon lab momentum of at least 350 MeV/c (the expected peak value) and (2) to the center-of-mass forward hemisphere, where the cross sections are anticipated to be both appreciably increased and more sharply peaked in the vicinity of the "N^*."

I. INTRODUCTION

THEORETICAL treatments of deuteron Compton scattering have been limited to impulse-approximation calculations.[1,2] In practice the deuteron amplitude is written as the product of the nucleon amplitude and a "sticking factor."[3] The manner in which this factorization is to be carried out is, however, still uncertain. Ambiguity related to the choice of nucleon momentum is just one of the difficulties. In any case, the process of factorization does not appear to be justifiable when the nucleon amplitude is dominated by

* This work was supported by the U. S. Office of Naval Research under Contract No. 1834(05).

[1] R. H. Capps, Phys. Rev. **106**, 1031 (1957), and references contained therein; R. H. Capps, *ibid.* **108**, 1032 (1957); M. Jacob and J. Mathews, *ibid.* **117**, 854 (1960); V. K. Fedyanin, Zh. Eksperim. i Teor. Phys. **42**, 1038 (1962) [English transl.: Soviet Phys.—JETP **15**, 720 (1961)].

[2] J. D. Fox, Ph.D. thesis, Washington University, 1964 (unpublished).

[3] G. F. Chew, Phys. Rev. **84**, 710 (1951); R. E. Cutkosky, in *Proceedings of the Tenth Annual International Conference on High-Energy Physics at Rochester, 1960*, edited by E. C. G. Sudarshan, J. H. Tincot, and A. C. Melissions (Interscience Publishers, Inc., New York, 1961), p. 236.

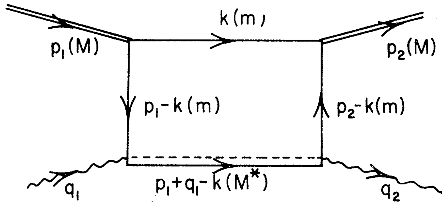

FIG. 1. The box graph. This is a Feynman diagram for the dominant (i.e., N^*) contribution (corresponding to the nearest anomalous singularity as discussed in Secs. II and III) to deuteron Compton scattering. p and q refer to deuteron and photon 4-momenta, respectively. The masses M, m, and M^* refer to deuteron, nucleon, and N^*, respectively: $M^*=m^*-i\Gamma/2$, where Γ is the full width of the $N^*(3,3)$ resonance. We use $m=0.940$, $M\simeq 1.878$, $m^*=1.240$, and $\Gamma=0.125$. The units are BeV.

a pole in the direct (energy) channel. For example, this procedure fails in the Thomson limit (low-energy threshold) as a direct consequence of the incorrect treatment of the nucleon-pole contribution.[4]

Recently, two separate photon-deuteron scattering experiments[2,5] have been carried out above the photopion threshold, in the region of photon lab momentum (k_L) of about 220 MeV/c. The main result is an apparent rise in the differential cross section of about a factor of $1\frac{1}{2}$ as k_L changes from 180 to 250 MeV/c. For $\theta_{\gamma\gamma}$ [photon center-of-mass (c.m.) angle] $\simeq$110 degrees,[5] the rise is somewhat steeper than at 135 deg,[2,5] the former giving a factor of $1\frac{1}{2}$ as k_L changes from 218 to 250 MeV/c.

These observations have been interpreted as the tail (low-energy side) of the $N^*(3,3)$ resonance—such an interpretation arising naturally out of the impulse-factorization (IF) approach. However, since the N^* appears as a pole in the direct channel of the photon-nucleon amplitude, we question the reliability of the factorization procedure in this energy region. This objection is best appreciated if one considers the unphysical case where the N^* width goes to zero. The IF method clearly gives a divergent result in this limit, whereas proper treatment of an intermediate N^* of real mass m^* should produce the finite effect of the opening of a new channel. (Qualitatively, the same reasoning applies in the case of a nonzero N^* width.)

But, if not through an IF type mechanism, how can an "N^* rise" be produced? It is our purpose here to suggest an alternative.

We propose that a peak in the deuteron Compton cross section can arise as a result of the appearance of a Landau[6] singularity in the so-called anomalous region of the scattering amplitude. The Feynman graph depicted in Fig. 1 (mentioned, but not quantitatively discussed by Cutkosky[3]) contains such a singularity, hereafter referred to as LSB. As a function of increasing photon lab momentum, LSB (the properties of which we will discuss fully in Sec. II) rapidly approaches the physical scattering domain just above the N^* production threshold, thus producing a resonance-like behavior of the amplitude. (Hereafter, by the expression "N^* region," we will mean the regions slightly above and slightly below the N^* production threshold.)

The notion of the dominance of LSB (i.e., the box graph of Fig. 1) will be used in Sec. III to derive an expression for the deuteron Compton cross section, which will be compared with the available experimental data above the photopion threshold. The result of this comparison, as will be seen, is most encouraging.

II. THE LANDAU SINGULARITY OF THE BOX GRAPH

The Landau singularity LSB, contained in the box graph of Fig. 1, is manifested in the scalar function

$$B(s,t)=\frac{(-i)}{(2\pi)^4}\int d^4k\frac{1}{[k^2+m^2][(p_1-k)^2+m^2][(p_2-k)^2+m^2][(p_1+q_1-k)^2+M^{*2}]}. \tag{II.1}$$

The invariants s and t are given by

$$s=-(p_1+q_1)^2\,,\quad t=-(p_1-p_2)^2. \tag{II.2}$$

The external 4-momenta p_1, p_2, q_1, and q_2 are identified in Fig. 1. Here k is an intermediate 4-momentum. M and m are the deuteron and nucleon masses, respectively, while M^* is the complex N^* mass;

$$M^*=m^*-i\Gamma/2. \tag{II.3}$$

The linear dependence of the four internal 4-momenta (i.e., the cyclic condition)[6] and the mass-shell restraints,

$$k^2=(p_1-k)^2=(p_2-k)^2=-m^2\,,\quad (p_1+q_1-k)^2=-M^{*2}\,, \tag{II.4}$$

determine the singularity structure of B in terms of s and t;

$$\begin{vmatrix} p_1^2 & p_1\cdot p_2 & p_1\cdot q_1 & p_1\cdot k \\ p_1\cdot p_2 & p_2^2 & p_2\cdot q_1 & p_2\cdot k \\ p_1\cdot q_1 & p_2\cdot q_1 & q_1^2 & q_1\cdot k \\ p_1\cdot k & p_2\cdot k & q_1\cdot k & k^2 \end{vmatrix}=0. \tag{II.5}$$

$(p_1^2=p_2^2=-M^2,\, q_1^2=q_2^2=0.)$

Multiplying out the determinant, we obtain

$$t=X(s)/P(s)\,, \tag{II.6}$$

[4] R. L. Schult and R. H. Capps, Phys. Rev. **119**, 377 (1960).

[5] R. S. Jones, H. J. Gerber, A. O. Hanson, and A. Wattenberg, Phys. Rev. **128**, 1357 (1962).

[6] L. D. Landau, Nucl. Phys. **13**, 181 (1959).

where

$$X(s)=4m^2(s-M^2)^2-4\Delta M^2(s-M^2)+4\Delta^2M^2, \quad \text{(II.7)}$$

$$P(s)=[s-(M^*-m)^2][s-(M^*+m)^2], \quad \text{(II.8)}$$

$$\Delta=M^{*2}-m^2. \quad \text{(II.9)}$$

In Fig. 2 we show the branch of the Landau curve [Eq. (II.6)] that approaches close to the physical region. (In drawing the curve, we have neglected the N^* width while using a mass of 1240 MeV. However, in all succeeding numerical work we use the complex value for the mass, M^*. This procedure for the treatment of a resonance in the intermediate state has been justified for a graph similar to that in Fig. 1 by Aitchison and Kacser.[7] Their reasoning applies equally well to our case.) The minimum of the curve or point of "closest approach" is

$$s_M=(m^2+M^{*2})/(1-2m^2/M^2), \quad \text{(II.10)}$$

$$t_M=X(s_M)/P(s_M)=16\gamma^2+O(\gamma^4/M^2), \quad \text{(II.11)}$$

where

$$\gamma^2=m^2-M^2/4. \quad \text{(II.12)}$$

Here γ is related to the deuteron binding energy B_E by

$$\gamma\simeq(mB_E)^{1/2}. \quad \text{(II.13)}$$

One observes the rapid approach to the physical region (hatched area) in going from the s threshold (corresponding to the opening of the N^* channel)

$$s_T=(m+M^*)^2, \quad \text{(II.14)}$$

to the "minimum point" s_M. As we will shortly demonstrate, this has the effect of producing a peak in B in the region between s_T and s_M, i.e., k_L in the region between 325 and 350 MeV/c.

The function $B(s,t)$ can be written as a single variable dispersion relation in t:[8]

$$B(s,t)=\frac{1}{\pi}\int_{t_M}^{\infty}\frac{\mathrm{Im}B(s,t')}{t'-t}. \quad \text{(II.15)}$$

We use the discontinuity given by[9]

$$2i\,\mathrm{Im}B(s,t)=\frac{(-i)(2\pi i)^3}{(2\pi)^4}\int\frac{d^4k}{(p_1+q_1-k)^2+M^{*2}} \times\delta(k^2+m^2)\delta((p_1-k)^2+m^2)\delta((p_2-k)^2+m^2). \quad \text{(II.16)}$$

Strictly speaking, Eq. (II.16) is valid only in the anomalous region (i.e., for $t<4m^2$); however, the error incurred in its use in the complete t region of integration is estimated to be very small, not more than a few percent for $s\simeq s_M$.

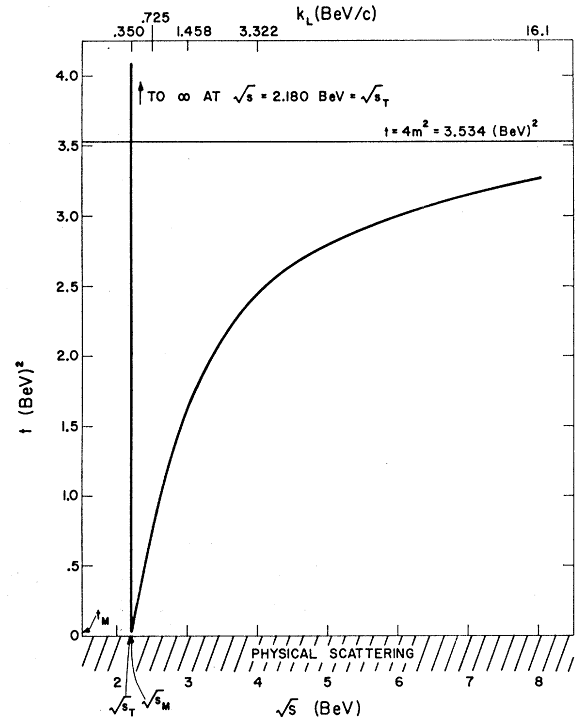

FIG. 2. The Landau singularity curve for the box graph with an N^*. For the purposes of this figure, the N^* is treated as a particle of real mass, $m^*=1.240$ BeV. s_T is the threshold (in s) for the opening of the N^* channel. (s_M, t_M) is the point of closest approach to the physical scattering domain (hatched area) in the (s,t) plane. The region $t_M\leq t\leq 4m^2$ is the anomalous region. k_L is the photon lab momentum, while $\sqrt{s}$ and $-t$ are the c.m. energy and the invariant momentum transfer squared, respectively.

Substituting Eq. (II.16) into Eq. (II.15), we can perform all the integrals in terms of "elementary functions," arriving at

$$B(s,t)=\frac{(-i)}{16\pi Z_2}\ln\frac{Z_1-Z_2}{Z_1+Z_2}, \quad \text{(II.17a)}$$

where

$$Z_1=[P(s)]^{1/2}(t_M-t)+it_M^{1/2}[X(s)-P(s)t_M]^{1/2}, \quad \text{(II.17b)}$$

$$Z_2=(-t)^{1/2}[X(s)-P(s)t]^{1/2}. \quad \text{(II.17c)}$$

Instead of the variables s and t ($\sqrt{s}$ is the total energy in the center-of-mass system; $-t$ is the momentum transfer squared), it is convenient to use the previously introduced variables k_L (the photon-lab momentum) and $\theta_{\gamma\gamma}$ (the angle between the incoming and outgoing photons in the c.m. system). The relations connecting the two sets of variables are

$$k_L=(s-M^2)/2M, \quad \text{(II.18)}$$

$$t=(s-M^2)^2(\cos\theta_{\gamma\gamma}-1)/2s. \quad \text{(II.19)}$$

[7] I. J. R. Aitchison and C. Kacser, Phys. Rev. **133**, B1239 (1964). See also: I. J. R. Aitchison, *ibid.* **133**, B1257 (1964).

[8] S. Mandelstam, Phys. Rev. **115**, 1741 (1959). J. D. Jackson, in *Dispersion Relations*, Scottish Universities' Summer School, 1960, edited by G. R. Screaton (Oliver and Boyd, Edinburgh, 1961), p. 1; R. Karplus, C. M. Sommerfield, and E. H. Wichmann, Phys. Rev. **111**, 1187 (1958); K. Nishijima, *ibid.* **126**, 852 (1962).

[9] R. E. Cutkosky, J. Math. Phys. **1**, 429 (1960).

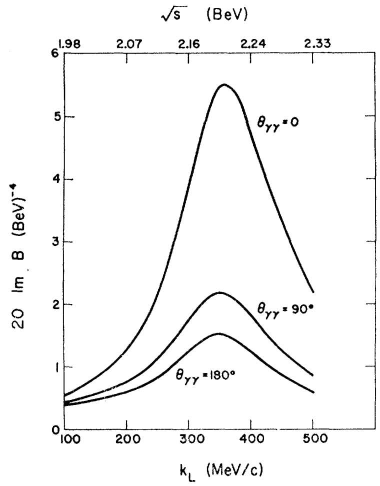

FIG. 3. The imaginary part of $B(s,t)$. B is given in Eqs. (II.17). k_L is the photon lab momentum; $\theta_{\gamma\gamma}$ is the photon scattering angle in the c.m. system and $\sqrt{s}$ is the total energy in the c.m. system.

To illustrate the behavior of $B(s,t)$ we show in Figs. 3 and 4 its imaginary and real parts, respectively, as functions of k_L for three different values of $\theta_{\gamma\gamma}$: 0, 90, and 180 deg. The 0-deg curve for ImB (corresponding to zero momentum transfer) exhibits a sharp peak at $k_L \sim 360$ MeV/c; but, as $\theta_{\gamma\gamma}$ changes toward backward angles, we observe a successive diminishing of the peak strength with a concomitant enlarging of the effective width. (The latter property represents a significant difference from the IF models where the predicted width in k_L for the imaginary part of the deuteron Compton amplitude is t-independent.) The interesting feature of the ReB curves is that each passes through zero for $k_L \sim 370$ MeV/c. Thus the phase of B passes through 90 deg near the peak of ImB, completing the simulation of "resonance" behavior.

III. THE DEUTERON COMPTON CROSS SECTION

In order to clearly demonstrate the effect of the Landau singularity LSB, and to avoid for the present the ambiguities and divergence difficulties inherent in the spin case,[10] we propose to treat all particles as scalars. We believe that spins are actually inessential to our purposes here, although it would undoubtedly be a significant step forward to be able to include them properly.

A second assumption we make is the dominance of the closest Landau singularity LSB, represented by the Feynman graph of Fig. 1. This means that in calculating the amplitude in the N^* region, all other contributions are neglected. The mass-shell properties of LSB given by Eqs. (II.4) allow us to replace the invariants at each of the four vertices (see Fig. 1) by coupling constants, independently known quantities. The calculation of the transition probability is thus reduced to perturbation theory with no free parameters.

The vertex couplings we use are $-i(4\pi)^{1/2}gm$ and $-i(4\pi)^{1/2}g^*em^*$ for the deuteron and photon vertices, respectively (see Fig. 1). Thus, the Compton cross section, in proton Thomson units $(e^2/m)^2$, can be written

$$\left(\frac{d\sigma}{d\Omega}\right)_{\text{c.m.}} \Big/ \left(\frac{e^2}{m}\right)^2 = \frac{4(2\pi)^2}{s} m^6 m^{*4} g^4 g^{*4} |B|^2, \quad \text{(III.1)}$$

where B is given by Eqs. (II.17). The "4" in the numerator is due to the summing of neutron and proton amplitudes.

g is obtained from a comparison with low-energy n-p scattering, extrapolated to the deuteron pole:

$$g^2 = \frac{32\gamma/m}{1-\rho\gamma}, \quad \text{(III.2)}$$

where ρ is the effective range of the deuteron, with the value 1.2 inverse pion masses (γ has the value $\frac{1}{3}$ of a pion mass). g^* can be estimated from proton Compton data with the formula

$$g^{*4} = (\Gamma^2/m^2)\sigma(N^*)/\pi, \quad \text{(III.3)}$$

where $\sigma(N^*)$ is the total proton Compton cross section at the N^* peak [in units of $(e^2/m)^2$], which was estimated from the data of DeWire *et al.*[11] Using their results at photon center-of-mass angles of 75, 90, and 120 deg, and photon lab energy ranging between 300 and 400 MeV, we obtain [see also Fedyanin of Ref. (1)]

$$\sigma(N^*) \simeq 10(8\pi/3). \quad \text{(III.4)}$$

Equations (III.3) and (III.4) thus give

$$g^{*4} \simeq (80/3)\Gamma^2/m^2. \quad \text{(III.5)}$$

In Figs. 5(a), (b) we show the k_L distributions for deuteron Compton scattering in the N^* region, using

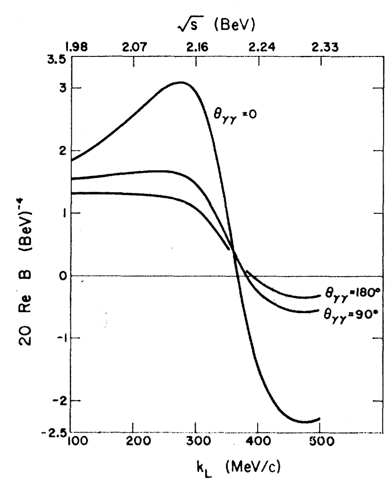

FIG. 4. The real part of $B(s,t)$. See the caption of Fig. 3.

[10] A possible way to approach the problem with spins included is suggested in a recent paper on the deuteron electromagnetic form factors: K. Dietz and M. Month, Phys. Rev. **152**, 1364 (1966). See also M. Month, *ibid.* **151**, 1302 (1966).

[11] J. DeWire, M. Feldman, V. L. Highland, and R. L. Littauer, Phys. Rev. **214**, 909 (1961).

the theoretical expression for the differential cross section given by Eq. (III.1).[12] The former uses $\theta_{\gamma\gamma}=135$ deg, while the latter is for $\theta_{\gamma\gamma}=110$ deg. The experimental points are taken from Refs. 2 and 5 as previously indicated.

IV. CONCLUSIONS

Our results, based on the remarkably simple expression (III.1) and displayed in Figs. 5(a), (b), adequately describe the limited experimental data. However, a further and significant test of the model we have proposed will come when the photon lab energy is experimentally extended over the N^* peak, and when the photon c.m. angle reaches the forward hemisphere. It is here, near the N^* peak and as close to the forward direction as possible, that we expect our model to be most accurate. As $\theta_{\gamma\gamma}$ goes to smaller angles, we predict (see Figs. 3 and 4): (1) a much sharper, resonance-like peak in the cross section near $k_L=350$ MeV/c; and (2) a much larger peak cross section.

On the theoretical side, we have presented here an interpretation of what we have termed the N^* effect in deuteron Compton scattering, an interpretation not based on the usual impulse-resonance (that is, IF) notion.[13] Our alternative obviates the difficulty when a pole exists in the direct channel of the nucleon amplitude by properly treating this "particle" as an intermediate state. Thus, we propose the box graph of Fig. 1 which contains a Landau singularity in the anomalous region of the deuteron-photon amplitude. This singularity comes very close (a distance of the order of the deuteron binding energy) to the physical scattering domain as k_L passes through the N^* region. With our simplified calculation, we have demonstrated that the process depicted in Fig. 1 does indeed simulate resonance behavior, however, with the interesting property that as the deuteron momentum transfer increases, its effective width enlarges, while the peak height significantly diminishes.[14]

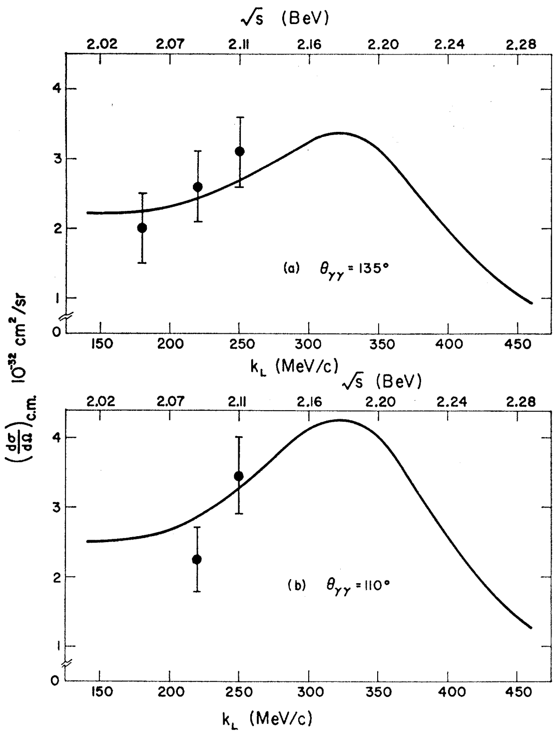

FIG. 5. The differential cross section in the center-of-mass system $(d\sigma/d\Omega)_{\text{c.m.}}$ for deuteron Compton scattering: (a) $\theta_{\gamma\gamma}=135$ deg; (b) $\theta_{\gamma\gamma}=110$ deg. We use the units 10^{32} cm²/sr, related to proton Thomson units by $(e^2/m)^2=2.35\times10^{-32}$ cm². The experimental data are taken from Ref. 2 (the 135-deg points) and Ref. 5 (the 110-deg points). The theoretical curves are obtained from Eq. (III.1). $\theta_{\gamma\gamma}$ is the photon c.m. scattering angle. k_L is the photon lab momentum, while $\sqrt{s}$ is the total energy in the c.m. system. In computing these curves, we have used a complex N^* mass: $M^*=m^*-i\Gamma/2$, with $m^*=1240$ MeV, and $\Gamma=125$ MeV.

[12] In obtaining the curves in Fig. 5 we have replaced the kinematic factor s of Eq. (III.1) by its value at the expected peak, $s_{\text{peak}}\simeq2(m^2+m^{*2})$.

[13] There is an interesting distinction between the interpretation of the N^* effect based on our approach and that based on IF models. The "sticking factor" of IF theory models contains the effects of the short-range part of the deuteron wave function. Another way of saying this is that the deuteron wave function is normalized independently of the "factored" photon-nucleon amplitude. On the other hand, the correspondence between the box graph of Fig. 1 and the nonrelativistic approach is such that only the long-range part of the wave function is included. That is, short-range effects do not, in our model, produce the N^*. This is perhaps interesting in the light of the following: A numerical calculation of the "factored Fig. 1" (not reported here) gives an increase in magnitude of the amplitude $B(s,t)$ by a factor of from two to three. The agreement with experiment (see Sec. III) using the factored $B(s,t)$ is exceedingly poor. However, it should be pointed out that if one were to *ad hoc* "normalize the deuteron form factor," i.e., include short-range effects, then the factored amplitude would, at least in order of magnitude, give a reasonable agreement with experiment. Although the significance of this is not clear, one of the points made in this paper is that the N^* effect should not be associated with short-range deuteron effects.

[14] Of course, the "sticking factor" of IF theories also produces a diminishing of the cross section as the momentum transfer increases. The N^* width is not, however, significantly altered.